ARTICLE   OPEN

Structural and functional connectivity in relation to executive functions in antipsychotic-naïve patients with first episode schizophrenia and levels of glutamatergic metabolites

Tina D. Kristensen [1 ✉], Karen S. Ambrosen [1], Jayachandra M. Raghava[1,2], Warda T. Syeda [3], Thijs Dhollander[4], Cecilie K. Lemvigh [1], Kirsten B. Bojesen[1], Anita D. Barber[5,6], Mette Ø. Nielsen[1,7], Egill Rostrup[1], Christos Pantelis [8], Birgitte Fagerlund [9,10], Birte Y. Glenthøj [1,7] and Bjørn H. Ebdrup[1,7]

Patients with schizophrenia exhibit structural and functional dysconnectivity but the relationship to the well-documented cognitive impairments is less clear. This study investigates associations between structural and functional connectivity and executive functions in antipsychotic-naïve patients experiencing schizophrenia. Sixty-four patients with schizophrenia and 95 matched controls underwent cognitive testing, diffusion weighted imaging and resting state functional magnetic resonance imaging. In the primary analyses, groupwise interactions between structural connectivity as measured by fixel-based analyses and executive functions were investigated using multivariate linear regression analyses. For significant structural connections, secondary analyses examined whether functional connectivity and associations with executive functions also differed for the two groups. In group comparisons, patients exhibited cognitive impairments across all executive functions compared to controls ($p < 0.001$), but no group difference were observed in the fixel-based measures. Primary analyses revealed a groupwise interaction between planning abilities and fixel-based measures in the left anterior thalamic radiation ($p = 0.004$), as well as interactions between cognitive flexibility and fixel-based measures in the isthmus of corpus callosum and cingulum ($p = 0.049$). Secondary analyses revealed increased functional connectivity between grey matter regions connected by the left anterior thalamic radiation (left thalamus with pars opercularis $p = 0.018$, and pars orbitalis $p = 0.003$) in patients compared to controls. Moreover, a groupwise interaction was observed between cognitive flexibility and functional connectivity between contralateral regions connected by the isthmus (precuneus $p = 0.028$, postcentral $p = 0.012$), all p-values corrected for multiple comparisons. We conclude that structural and functional connectivity appear to associate with executive functions differently in antipsychotic-naïve patients with schizophrenia compared to controls.

INTRODUCTION

The dysconnectivity hypothesis posits that disturbances in both structural and functional connectivity are central and interdependent aspects of the pathophysiology of schizophrenia[1,2]. While evidence supports overlapping anatomical and functional dysconnectivity in patients[3], the relationship between these modalities is complex[4], and studies examining the combined interplay with cognitive functions are sparse.

Structural dysconnectivity as measured by white matter (WM) alterations has been associated with clinical symptoms[5], cognition[6], and disease course in schizophrenia[7]. Diffusion weighted imaging (DWI) is a non-invasive magnetic resonance imaging (MRI) technique used to measure WM properties in vivo. Common methods for modelling MRI data, such as diffusion tensor imaging (DTI), have been extensively applied to investigate WM[8]. Although derived measures such as fractional anisotropy are sensitive indicators of WM organization, they are nonspecific to the underlying microstructure, are confounded by partial volume effects of grey matter and cerebrospinal fluid and cannot resolve fibre orientation or the presence of crossing fibres at the conventional spatial resolution of DWI data[9].

To address these limitations, new approaches as fixel-based analyses (FBA) have been developed, providing more biologically specific micro- and macrostructural measures of WM[10,11]. A "fixel" refers to each individual fibre-population within a voxel, and FBA enables the estimation of orientations for multiple fiber populations within a single voxel[10]. Thus, the FBA-derived measure of fibre density (FD) captures microstructural information proportional to the total intra-axonal volume of a specific fibre population within a voxel. At a macrostructural level the morphological measure of fibre-bundle cross-section (FC) reflect the total cross-sectional size of an individual fibre bundle[10]. The combined measure of fibre density and fibre-bundle cross-section (FDC) integrates the properties of FD and FC, providing a metric sensitive to both intra-axonal volume and the cross-sectional size of a specific fibre bundle[12] (see Supplementary Figure S1 for illustration). Decreases in fixel-wise metrics seem to indicate neurodegenerative processes[13,14], which, along with significant

[1]Center for Neuropsychiatric Schizophrenia Research, Mental Health Centre Glostrup, Copenhagen University Hospital, Glostrup, Denmark. [2]Functional Imaging Unit, Department of Clinical Physiology, Nuclear Medicine and PET, Rigshospitalet, Glostrup, Denmark. [3]Melbourne Brain Center Imaging Unit, Department of Radiology, University of Melbourne, Parkville, VIC, Australia. [4]Developmental Imaging, Murdoch Children's Research Institute, Parkville, VIC, Australia. [5]Department of Psychiatry, Zucker Hillside Hospital and Zucker School of Medicine at Hofstra/Northwell, Northwell, NY, USA. [6]Center for Psychiatric Neuroscience, Feinstein Institute for Medical Research, Manhasset, NY, USA. [7]Department of Clinical Medicine, Faculty of Health and Medical Sciences, University of Copenhagen, Copenhagen, Denmark. [8]Department of Psychiatry, University of Melbourne and Melbourne Health, Parkville, VIC, Australia. [9]Child and Adolescent Psychiatry, Mental Health Centre, Copenhagen University Hospital, Hellerup, Copenhagen, Denmark. [10]Department of Psychology, University of Copenhagen, Copenhagen, Denmark. ✉email: tina.dam.kristensen@regionh.dk

neurodevelopmental factors[15,16], have been proposed as contributing elements to the pathophysiology of schizophrenia[17,18].

In a previous FBA-study, we identified aberrant WM fibres and associations with clinical symptoms in patients with first episode psychosis[19]. In the present study with a partially overlapping sample, we additionally included cognitive measures, and resting state functional magnetic resonance imaging (rs-fMRI) data from patients and healthy controls (HC), see flowchart Supplementary Figure S3 for detailed description of data inclusion.

Executive functions (EF) encompass a range of cognitive processes, including planning, flexibility, working memory, and fluency[20]. EF regulate cognition, behaviour and emotions while enabling decision making and goal-directed responding[21]. Cognitive deficits are core symptoms of schizophrenia[22,23], with deficits in EF proposed as a cognitive endophenotype[24]. Associations between EF and structural connectivity in patients with schizophrenia are documented, particularly involving prefrontal dysfunctions and dysconnectivity[25,26]. However, the specific microstructural properties underlying these cognitive impairments and their functional implications remain unclear[27], and previous studies have typically investigated more chronic patients receiving antipsychotic treatment, potentially confounding results. Given the central role of executive dysfunctions in schizophrenia, investigating associations between EF and structural and functional connectivity in antipsychotic-naïve patients with first-episode schizophrenia may provide valuable insight into underlying disease mechanisms, clarifying the complex interplay between cognition and multiple neurobiological modalities.

Aims

The present study compares antipsychotic-naïve, first-episode patients with schizophrenia to HCs using fixel-based measures and EF. Drawing upon our previous study using FBA in a partly overlapping sample[19], we expected that patients would have lower FD and FC in corpus callosum, along with overall EF impairments when compared to HCs.

In the primary analyses we examined group difference and interactions between WM characteristics (FD, FC, and FDC) and EF. In the secondary analyses we examined group differences in the functional connectivity (rs-fMRI) between those regions of interest (ROIs) connected by WM tracts identified in the primary analyses. Additionally, potential interaction effects on the groupwise associations between functional connectivity and the EFs, and the tract-wise FBA measures (FD, FC; and FDC) identified in the primary analyses are examined. See the a priori analysis-plan in Supplementary Fig. S2 for details.

METHODS

Data was acquired as part of two consecutive studies (PECANS I and II) conducted in the Capital Region of Copenhagen, Denmark, in the period 2008-2019[28,29]. The studies comply with the Committee on Biomedical Research Ethics (H-D-2008-088, H-3-2013-149) and with the Helsinki Declaration of 1975. Both studies were registered at Clinicaltrials.gov (NCT01154829, and NCT02339844). All participants provided oral and written informed consent prior to inclusion in the study.

Participants

Patients aged 18-45 years were recruited from psychiatric hospitals and outpatient clinics. Patients met the criteria for the non-affective psychotic spectrum (DF2x) according to the International Classification of Diseases 10th edition (ICD-10). Diagnostic status of patients was confirmed using the Schedules for Clinical Assessment in Neuropsychiatry (SCAN), version 2.1[30]. Trained raters assessed psychopathology using the Positive And Negative Syndrome Scale (PANSS)[31]. In total, 109 antipsychotic-naïve patients with diagnoses of schizophrenia or psychosis were included. Exclusion criteria for patients were previous treatment with antipsychotics or methylphenidate, a current diagnosis of drug abuse or dependency according to ICD-10, treatment with antidepressant medication within the last month, involuntary admission or treatment, or severe physical illness. Previous substance abuse, and current occasional substance and benzodiazepine use were accepted for patients. In the current analyses, we only included 64 patients with schizophrenia (DF20.x) to increase sample homogeneity, and excluded participants with life substance abuse, see Supplementary Fig. S3 for inclusion flow chart. Furthermore, we included new data from resting state f-MRI and cognitive testing of executive functions from HCs and patients.

118 HCs were recruited using online advertising and matched to patients based on age, sex, and parental socioeconomic status. Exclusion criteria for HCs were any physical or mental illness, having a first degree relative with psychotic symptoms, or substance abuse during the last 3 months before inclusion. All participants reported quantity and frequency of their substance use (alcohol, tobacco, cannabis, stimulants, hallucinogens, opioids, other illicit drugs) and provided a urine drug-screen test (Rapid Response, Jepsen HealthCare, Tune, DK). A neuroradiologist examined all MRI scans and participants with overt MRI pathology were excluded. Figure S3 displays details of the recruitment and inclusion process for patients and healthy controls.

Assessments

Cognitive assessments. A comprehensive neuropsychological battery was administered by trained personnel, examining a broad range of cognitive domains as proposed by MATRICS (Measurement and Treatment Research to Improve Cognition in Schizophrenia)[32]. In the current study we report data from five a priori selected tests: DART and four tests assessing EF. The Danish version of the National Adult Reading Test (DART)[33] was used to obtain estimates of premorbid intelligence. The EF tests were selected based on i) previous studies in patients with schizophrenia reporting associations between WM and EF[20]; and ii) studies employing latent variable analyses reporting the shared and unique contribution of various EFs[34,35]. Planning and cognitive flexibility were assessed using Stockings of Cambridge (SOC, problems solved in minimum moves) and Intra-Extra Dimensional Set Shift (IED, total errors adjusted) from the Cambridge Neuropsychological Test Automated Battery (CANTAB)[36]. Verbal working memory (digit sequencing) and verbal fluency were tested using Brief Assessment of Cognition in Schizophrenia (BACS)[37].

Image acquisition. Acquisition parameters for DWI data are described in details elsewhere[19]. Briefly, the MRI scans were acquired with a Philips Achieva 3.0 T MRI scanner. In the first cohort an 8-channel SENSE Head Coil was used, while a 32-channel Head Coil was used in the second cohort. Diffusion weighted images were obtained using single shot spin-echo echo-planar imaging with 5 non-diffusion-weighted ($b = 0$ s/mm^2) and 30 diffusion weighted ($b = 1000$ s/mm^2) in non-collinear directions. The acquisition matrix was 128×99, FOV $= 240 \times 240$ mm^2, number of slices $= 75$, slice thickness $= 2$ mm (no gap), reconstructed voxel dimensions $= 1.88 \times 1.88 \times 2$ mm^3, TR/TE $= 7035/68$ ms, parallel imaging SENSE factor $= 3$(AP), flip angle $= 90°$, and the total scan duration was 522 s.

In the first cohort, functional images were acquired using a T2*-weighted echo planar imaging sequence (TR $= 2$ s, TE $= 25$ ms, flip angle $= 75°$). The matrix size was $128 \times 128 \times 38$ and the field of view was $230 \times 230 \times 128$ mm, resulting in a voxel size of $1.8 \times 1.8 \times 3.4$ mm. The acquisition resulted in 300 volumes, and the total scan time was 10 min. In the second cohort, functional images were acquired using a T2*-weighted echo planar imaging sequence (TR $= 3034$ ms,

TE = 35 ms, flip angle = 90º). The matrix size was $80 \times 80 \times 37$ and the field of view was $230 \times 126 \times 230$ mm³, resulting in a voxel size of $2.9 \times 2.9 \times 3.4$ mm³. The acquisition resulted in 200 volumes, and the total scan time was 10 min.

For anatomical reference, high-resolution three-dimensional T1-weighted structural brain images were acquired sagittally using the following parameters: acquisition matrix = 304×299, field of view (FOV) = 240×240 mm², number of slices = 200, slice thickness = 0.8 mm, reconstructed voxel dimensions = $0.75 \times 0.75 \times 0.80$ mm³, TR/TE = 10/4.6 ms, inversion time = 964 ms, flip angle = 8º, total scan duration = 10.01 min.

Image processing. Structural T1 scans were processed using Freesurfer (version 7.1.1) software. Sequence Adaptive Multimodal SEGmentation (SAMSEG) tool was used to calculate intracranial volumes (ICV) for all the subjects[38].

DWI data were processed using a previous described pipeline[19]. Briefly, images were denoised[39] and corrected for bias[40] and eddy currents[41,42] using FMRIB diffusion tool box (part of FSL 6.00)[43,44] and MRtrix3Tissue (https://3Tissue.github.io)[40]. The data were resampled to 1.3 mm3 resolution using cibic b-spline interpolation[40], and a whole brain mask were generated using 'dwi2mask'. Single-Shell 3-Tissue CSD (SS3T-CSD) was performed for each subject to obtain WM-like fiber orientation distribution (FOD) maps[45]. FODs were normalized and registered non-linearly to the population template[46,47] using 'mtnormalise'[10,40]. FODs were segmented to produce fiber-specific fixels and were reoriented[10,48]. Apparent FD, FC, and the combined measure of FDC (Fiber density and cross-section) across all WM fixels were computed for each subject, and we performed a whole brain probabilistic tractography on the FOD template using the spherical-deconvolution informed filtering of tractograms (SIFT)[48]. After SIFT filtering, the whole brain tractogram was smoothed, and statistical inference was obtained based on connectivity-based fixel enhancement[49].

Resting-state functional images were preprocessed using FSL FEAT version 6.0. Motion correction was performed with MCFLIRT[42], and brain extraction with BET in FSL were applied[50]. Spatial smoothing using a 5 mm Gaussian kernel enhanced signal-to-noise ratio. High-pass filtering (200 s) removed low-frequency noise and drift. Registration to the T1-weighted anatomical image was achieved using FLIRT[51] and FNIRT[52] to the MNI152 standard brain template. Motion-related artifacts and physiological noise were removed with ICA-AROMA[53,54].

Desikan-Killiany cortical parcellation[55] and subcortical segmentation in FreeSurfer space were registered to the native anatomical space using *mri_convert* with nearest neighbor interpolation and converted to RAS coordinates for alignment with FSL. Linear registration aligned the native structural image to the high-resolution structural image in FSL, and the transformation was applied to the Desikan-Killiany segmentation to obtain segmentation in functional space.

Average timeseries were extracted from those ROIs identified in the primary WM analyses. This included four bilateral ROIs (isthmus cingulate, precuneus, postcentral, and superior parietal regions), and eight left hemisphere ROIs (thalamus, lateral orbitofrontal, rostral middle frontal, superior frontal, pars opercularis, pars orbitalis, pars triangularis, and rostral anterior-cingulate regions). Timeseries were motion-corrected using the Friston 24-parameter model, which includes six head motion parameters, six head motion parameters from the previous time point, and their corresponding squared items[56]. Additionally, timeseries were corrected for the global signal.

Additional details on processing of DWI and rs-fMRI data can be found in Supplementary Table S4 and Text S4.

Statistical analyses

Analyses of descriptive data were performed using SPSS version 25.0, Armonk, NY and reported with count, percent, means and standard deviations. Distributions of continuous data were tested for normality by visual inspection of histograms, and outliers were examined. When skewness was detected, cognitive data were normalized with square root transformation, and standardized Z-scores were calculated for between group- and correlation analyses. Group differences on nominal data were tested using Pearson's χ^2 test or Fisher's Exact Test, while ordinal data were tested using the Mann-Whitney U test or Fisher's Exact Test as appropriate. Group differences on continuous data was tested using ANOVA. Cognitive data were bootstrapped to attain confidence intervals.

The primary FBA was performed using MATLAB software (version 2017b). For each subject, FD, FC, and FDC were computed across all white matter fixels. We conducted whole-brain analysis using General Linear Modeling (GLM) to compare patients with controls and to test associations between EF and fixel-based measures. In a multivariate model, the fixel-wise measures of apparent FD, FC, and FDC were entered as predictors, and the 4 EF as outcome. The effect of a major scanner upgrade, as well as potential random effects of cohort were examined by both visually plotting global mean FD across scandate and scanner upgrade, as well as testing the effect of scandate and cohort. As we observed a significant negative correlation (RHO = −0.18; $p = 0.02$) between global FD and scandate and a drop in global FD after major scanner upgrade, we added cohort and scanner upgrade as covariate, along with age, sex, cohort, ICV, and six motion parameters. Family-wise error (FWE) corrected p-values were calculated for each fixel using non-parametric permutation testing with 5000 permutations with a significance threshold of $p < 0.05$[57]. To obtain t statistics, mean fixel-based values were extracted from the significant clusters and tested post hoc.

ROIs for the secondary analyses were selected based on the results from the primary analyses. The functional connectivity between cortical grey matter ROIs connected anatomically by the WM tracts identified in the primary analyses were estimated by first extracting time-course of activity for each ROI and then computing the Pearson correlation between ROI pairs[58]. The correlation coefficients were Fisher transformed. We tested a potential groupwise interaction effect of the association between functional connectivity between the ROIs and the EFs that associated significantly in the primary analyses. Results were corrected for multiple comparisons using FWE, and we included six motion parameters, global signal, age, sex, cohort, and major scanner upgrade as covariates.

RESULTS

We included 64 antipsychotic-naïve patients with first-episode schizophrenia (DF20.x) and 95 HC. Demographic and clinical characteristics are reported in Table 1. Participants were balanced on age, sex, parental socioeconomic status, and handedness. Patients had a higher recreational use of alcohol ($p = 0.019$), nicotine ($p = 0.003$), cannabis ($p < 0.001$), and other illicit drugs (opioids, stimulants, hallucinogens).

Patients presented with significant lower premorbid IQ (DART, $p = 0.012$, $F = 6.544$), impaired cognitive flexibility (IED, $p < 0.001$, $F = 11.648$) and planning abilities (SOC, $p = 0.006$, $F = 7.927$), impaired verbal working memory (digit sequencing $p < 0.001$, $F = 15.667$), and verbal fluency ($p < 0.0001$, $F = 36.683$) (see Fig. 1 for illustration of the groupwise distribution).

Structural connectivity and the associations to executive functions

We observed no group differences on FBA measures but identified a groupwise interaction on the association between planning abilities (SOC) and FC in a cluster (1846 voxels) located to the left anterior thalamic radiation (l-ATR), t(3,155) = 2.768, $p = 0.006$. The

Table 1. Sociodemographic, clinical, and cognitive data.

Variable mean (S.D.)/Percent	Controls (N = 95)	Patients (N = 64)	Significance group effect
Age, years, mean (SD)	24 (5)	24 (6)	$p = 0.88$
Sex			$p = 0.34$
Male	55%	50%	
Female	45%	50%	
Parental SES high/middle/low, %	33/53/15%	32/49/19%	$p = 0.76$
Handedness			$p = 0.19$
FUNCTIONAL LEVEL (GAF TOTAL)	na	36 (10)	-
PANS POSITIVE	na	19 (4)	-
PANSS NEGATIVE	na	19 (7)	-
PANSS GENERAL	na	38 (9)	-
PANSS TOTAL	na	76 (17)	-
SUBSTANCES, % (never tried/ tried few times/ use regularly/ harmful use)			
Alcohol	2.1/7.4/90.4/0.0	5.3/24.6/61,4/8.8	**$p < 0.001$**
Nicotine	50.5/31.2/15.1/3.3	39.7/17.2/34.5/8.6	**$p = 0.010$**
Cannabis	41.5/52.1/6.4/0.0	32.8/43.1/17.2/6.9	**$p = 0.008$**
Opioids	96.8/3.2/0.0/0.0	79.3/19.0/1.7/0.0	**$p = 0.002$**
Stimulants	87.0/13.0/0.0/0.0	67.9/28.6/3.6/0.0	**$p = 0.009$**
Hallucinogens	95.7/4.3/0.0/0.0	88.9/11.1/0.0/0.0	**$p = 0.112$**
Other drugs	97.6/2.4/0.0/0.0	90.0/10.0/0.0/0.0	**$p = 0.085$**
COGNITION, mean (SD)			
Estimated premorbid intelligence	22.81 (5.97)	19.74 (8.57)	**$p = 0.01$**
Planning	10.34 (1.32)	9.53 (2.21)	**$p = 0.006$**
Cognitive Flexibility	6.12 (8.31)	12.90 (16.21)	**$p < 0.001$**
Verbal Working Memory	23.09 (3.52)	20.57 (4.30)	**$p < 0.001$**
Verbal Fluency	66.14 (12.60)	52.41 (15.10)	**$p < 0.001$**

Significant effect of group is marked in bold.
GAF Global assessment of Functioning Scale, *N* number, *PANSS* Positive And Negative Symptom Scale, *SD* standard deviation, *SES* socio-economic status.
Cognitive tests: Estimates of premorbid intelligence were obtained using the Danish version of Dutch adult reading test (DART). Planning and cognitive flexibility were assessed using Stockings of Cambridge (SOC, problems solved in minimum moves) and Intra-Extra Dimensional Set Shift (IED, total errors adjusted) from the Cambridge Neuropsychological Test Automated Battery (CANTAB). Verbal working memory (digit sequencing) and verbal fluency were tested using Brief Assessment of Cognition in Schizophrenia (BACS).

correlation between planning and FC was positive in patients, and negative in HCs, see Fig. 2 for details.

Furthermore, we found a groupwise interactions on the association between cognitive flexibility (IED) and FC located to isthmus of corpus callosum (cluster sized 244 voxels); as well as FD and FDC located to left cingulum (three clusters sized 80, 24, and 16 voxels), $t(3,155) = 1.986$, $p = 0.049$ corrected. The association between cognitive flexibility and FD, FC and FDC were positive in patients, and negative in HCs. See Supplementary Table S5 for specifics on location and interaction coefficients.

Functional connectivity and the associations to executive functions

The grey matter ROIs connected via the major WM tracts identified in the primary analysis were:

a) l-ATR connecting the thalamus with prefrontal ROIs, such as the lateral orbitofrontal, rostral middle frontal, superior frontal, pars opercularis, pars orbitalis, pars triangularis, and rostral anterior-cingulate regions. We tested the group difference on the functional connectivity between thalamus and the ROIs and found that patients had increased functional connectivity between left thalamus and pars opercularis ($t(3,155) = 3.052$, $p = 0.011$ corrected) and pars orbitalis ($t(3,155) = 3.499$, $p = 0.003$ corrected), respectively, when compared to HCs, see Fig. 3 for illustration and Supplementary Table S6_B for details.

Next, we tested the groupwise association between the EF and the functional connectivity between ROIs. No significant interaction effects were observed after correction (see Supplementary Table S6_A for details).

b) Isthmus of the corpus callosum connecting the parietal lobules between hemispheres. The term homotopic connectivity[59] denotes the functional connectivity across hemispheres as measured by directly correlating activity of a region in one hemisphere to the corresponding mirror region in the contralateral hemisphere[60]. Hence, we examined the homotopic connectivity between isthmus cingulate, precuneus, postcentral, and superior parietal mirror regions. No group difference in the functional connectivity between the homotopic ROIs was observed.

Testing the groupwise association between the EF and the functional connectivity between the homotopic ROIs we identified a groupwise interaction on the association between IED and the homotopic connectivity between the precuneus regions ($t(3,155) = 2.384$, $p = 0.03$ corrected). Increased homotopic connectivity between the precuneus regions was correlated with reduced cognitive flexibility in HCs, but not in patients.

Additionally, we identified a groupwise interaction on the association between IED and the homotopic connectivity between the postcentral regions ($t(3,155) = 2.90$, $p = 0.012$ corrected). Increased homotopic connectivity between the postcentral regions was correlated with higher IED in HCs (RHO 0.369, $p < 0.005$), see Fig. 3 for illustration.
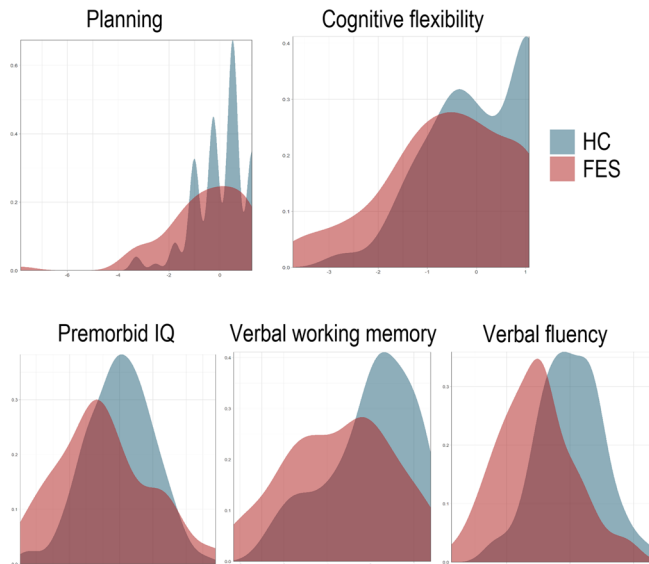
Fig. 1 Executive functions. Illustrates the density plots of the groupwise distribution of Z-Scores on the x-axis across executive functions, comparing patients with first episode schizophrenia (FES) in red plots with healthy controls (HC) in blue plots.

DISCUSSION

In a uniquely unconfounded sample of antipsychotic-naïve patients with first-episode schizophrenia and without any substance abuse, we observed groupwise interaction effects in the association between the EF of planning and FD of the lATR; as well as cognitive flexibility and FC of the isthmus. Furthermore, secondary analyses of functional connectivity elucidated the implications of the divergent associations between EF and connectivity in patients.

As expected, patients demonstrated impaired EF across all tests with moderate to large effect sizes. However, in the groupwise interaction analysis on the associations between EF and FBA measures, only planning and cognitive flexibility tested significant. Notably, all associations between fibre metrics and cognitive functions were positive in patients, with increased FD, or larger FC associated with better performance on EF in contrast to HC.

The positive association between planning and FD of lATR suggest that higher fibre density may support planning abilities in patients, which is consistent with previous studies in patients with schizophrenia[61-63]. The ATR is a projection tract which anatomically connects the thalamus with prefrontal cortex, known to be involved in EF[64]. Notably, the functional processes involved in planning are mainly mediated by the prefrontal cortex[65]. A recent review provided substantial evidence linking prefrontal hypoactivation to impaired cognitive control, including EF[66]. No
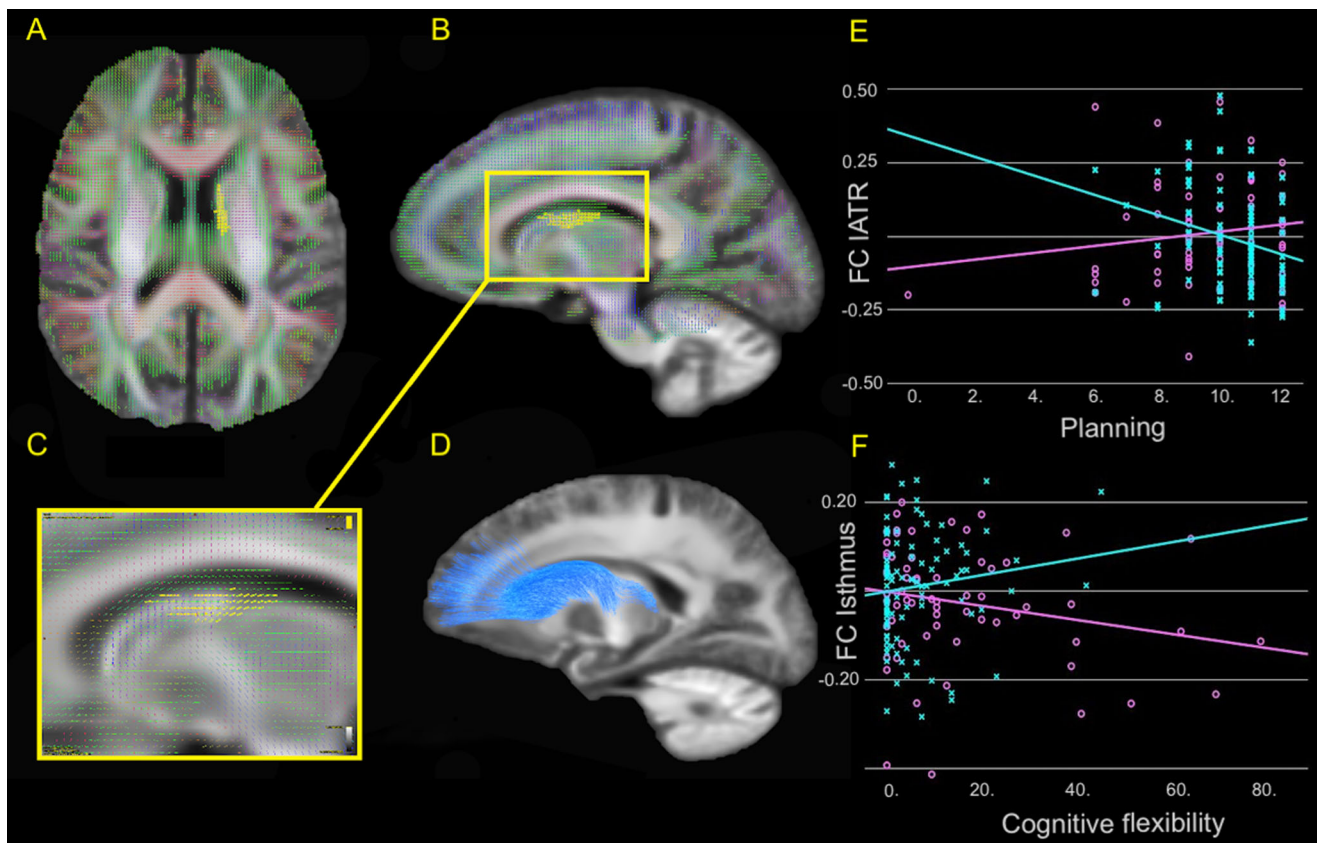

Fig. 2 Group-wise interaction between structural connectivity and executive functions. A Illustrates the area of the left anterior thalamic radiation (lATR) in an axial plane where the group-wise interaction on the association between planning abilities and fibre-bundle cross-section (FC) was located. **B** Displays the location of the significant area in lATR in a sagittal plane (all images presented in radiological orientation). **C** Shows the significant fixels coloured yellow, indicating the direction of the significant fibres, precluding nonsignificant crossing fibres within the voxels. **D** Illustrates the lATR tract using the John Hopkins University white matter tractography atlas. **E** Scatterplots illustrates the distribution of FC in lATR on the y-axis and planning abilities scores on the x-axis. **F** Shows the distribution of FC in Isthmus on the y-axis and cognitive flexibility scores on the x-axis. The groupwise interaction effect on the association is depicted with turquoise lines for controls, and purple lines for patients.
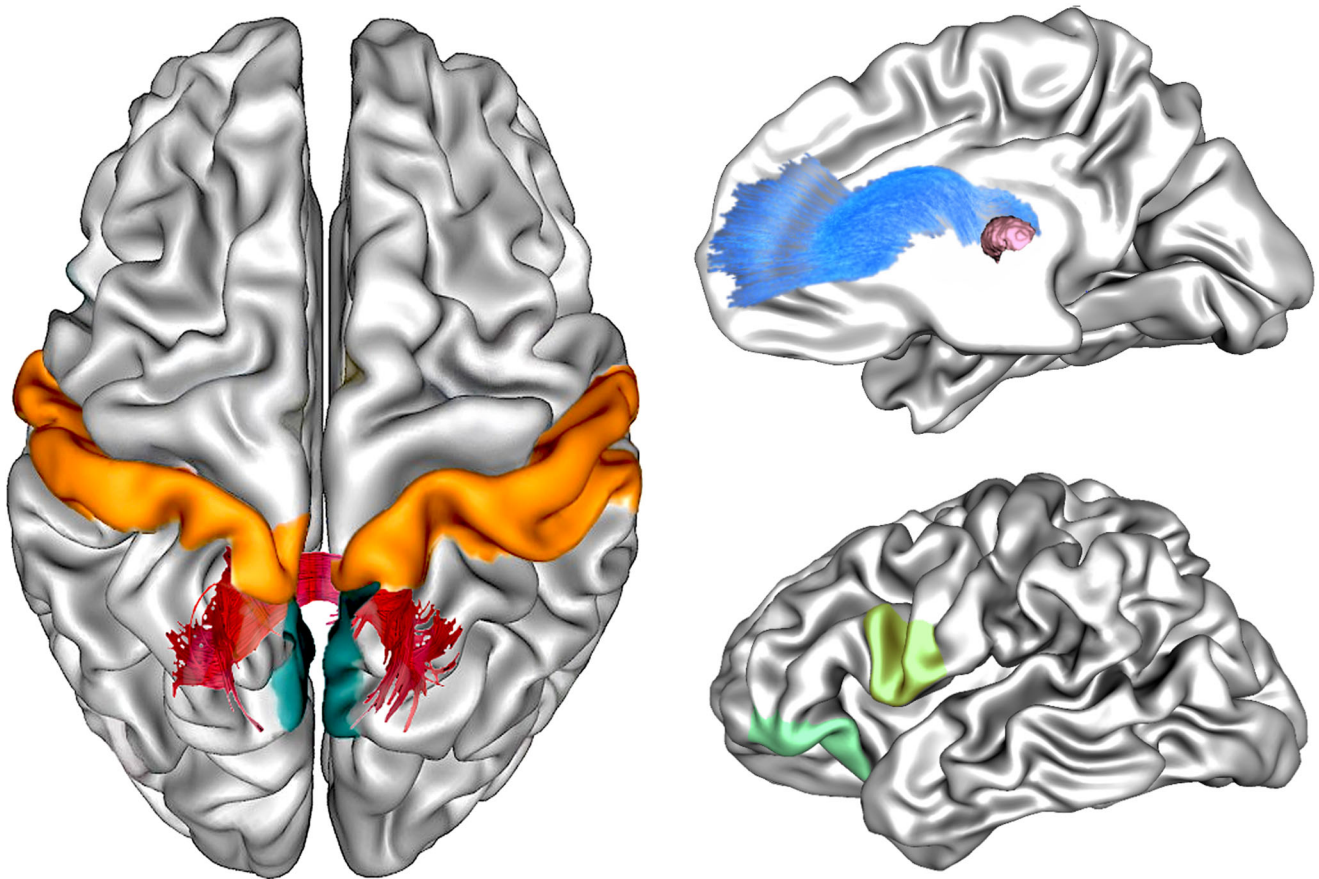
Fig. 3 Group-wise interaction between functional connectivity and executive functions. Left Panel illustrates the location of the groupwise interaction effect on the association between cognitive flexibility and fibre-bundle cross-section (FC) in the Isthmus (dark red). In the homotopic grey matter regions connected by the Isthmus, a groupwise interaction between cognitive flexibility and the functional connectivity between the precuneus regions (dark green) and the postcentral regions (orange) were identified. Right Panel (top) illustrates the left anterior thalamic radiation (lATR, blue). A groupwise interaction effect on the association between planning and fibre-bundle cross-section (FC) were identified. The lATR connects thalamus (pink) to prefrontal grey matter regions. Post hoc analysis revealed significantly different functional connectivity between the thalamus and left pars opercularis (light-green), and left pars orbitalis (green) in patients compared to controls.

correlations between planning and functional connectivity survived correction for multiple comparisons in our secondary analyses, but patients exhibited increased left lateralized functional connectivity between the thalamus and specific prefrontal regions, namely pars orbitalis and pars opercularis. We observed that the thalamocortical connectivity was increased in patients compared to HC. This finding may appear contra-intuitive, as reduced thalamic-prefrontal connectivity previously has been associated with cognitive deficits and more severe symptomology in patients with psychosis[67]. However, previous studies have also reported an overall asymmetry of the lateralized functional connectivity across the psychosis spectrum[68,69], where the specific directionality (hypo- or hyper-activation) appeared dependent on the sample and tract of interest[70]. Moreover, the distinct functional nuclei of thalamus may drive hypo- or hyperconnectivity respectively, dependent on the specific anatomical connections, making interpretations of the averaged connectivity across thalamic subregions difficult[71].

Cognitive flexibility is consistently found to be disrupted in patients with schizophrenia[72], and influenced by illness state, clinical profile[73], and antipsychotic medication[74]. While task based or rs-functional MRI studies on cognitive flexibility are common[73], studies examining WM correlates of cognitive flexibility are less frequent. Impaired WM of the middle cerebellar peduncles has been associated to poorer cognitive flexibility in patients with schizophrenia[75]. In our present study, the main localization for the interaction between cognitive flexibility and FC was within the isthmus of CC. Our results indicate that increased FC is associated with more cognitive flexibility in patients, which correspond with previous associations of reduced FC with brain atrophy and degeneration[10]. Consistent with our findings, a recent study on WM integrity reported deceased FA in CC associated with poorer cognitive flexibility in patients in later clinical stages of mental disorders, such as psychotic disorders[76].

Both SOC and IED are complex higher-order tasks that rely on the coordinated interaction and information transfer across multiple processing stages within extensive brain networks[77,78]. CC play a crucial role in integrating and synchronizing large scale neuronal activity across hemispheres[79,80]. The size of CC affects the balance between local and global interference[81], with larger callosal axons facilitating the interhemispheric synchronization of activity between contralateral cortical regions and supporting global processing[82]. The positive correlation between FC in isthmus and cognitive flexibility observed in patients suggest that better cognitive flexibility may be associated with microstructural properties supporting increased information transfer between hemispheres, indicative of greater reliance on global processing[83]. Notably, psychosis spectrum disorders have been linked to a preference for global over local cognitive processing[84].

We identified a groupwise interaction effect on the association between cognitive flexibility and the homotopic connectivity of the postcentral and precuneus regions, respectively. Specifically, better cognitive flexibility in HCs was strongly associated with increased homotopic connectivity between postcentral regions, whereas more cognitive flexibility in patients was associated with increased homotopic connectivity between precuneus regions. Hence, more cognitive flexibility was associated with increased homotopic connectivity in both patients and HCs, albeit within different functional networks.

Precuneus, located in the posteromedial parietal lobe, is involved in broader functional networks implicated in EF, including flexibility[85,86], and serves as a key structural hub of the default mode network (DMN)[87,88]. Studies have documented DMN hyperactivity in, drug naïve patients, emphasizing its relevance in the neurobiology of schizophrenia[89], although the underlying mechanisms remain unclear[90]. Our findings align with previous research indicating altered precuneus engagement in patients with schizophrenia. Mashal et al. used task-based fMRI to demonstrate that patients recruited precuneus to compensate for deficits in cognitive processing[91]. Our results support this observation, suggesting that patients rely on different, or less specialized networks involving precuneus for cognitive processing. Likewise, Wang et al. examined deficits in cognitive flexibility in patients with schizophrenia using task-based functional connectivity, and reported less efficient information transfer during task-processing[77], implying reduced cognitive flexibility despite compensatory activation of more global networks. In support of this speculation, one study reported that cognitive flexibility in healthy adults mainly relied on specialized lateralized processing[92], while increased global interhemispheric processing constrained cognitive flexibility[93].

Contrary to expectations, patients did not exhibit reduced FBA measures compared to HC. In a previous study with a partially overlapping sample, we found reduced FD in corpus callosum among patients with first-episode psychosis compared to HC[19]. We attribute the discrepancy in findings between studies to the reduced sample size in the current study, which excluded participants with substance abuse and missing cognitive data. In a confirmatory post hoc test, we found that the mean percentage effect size of FD in corpus callosum of patients compared to controls was similar in the previous study (3.5%) and in the current study (3.6%).

Concluding, we have observed how structural and functional connectivity appear to subserve EF differently in antipsychotic naïve patients with first-episode schizophrenia. Patients may engage compensatory global networks, yet EF remain reduced compared to HCs.

A major strength of this study is the unique sample of antipsychotic naïve patients with first-episode schizophrenia without any substance abuse, which enables high internal validity of data due to the lack of confounding effects from medication and duration of disease. However, several limitations must be considered. One methodological challenge arises from the pooling of data from independent cohorts. Variations in scanner parameters and random effects of study cohorts can serve as potential confounders in MRI-studies[94]. To address this, we thoroughly investigated the effects of a major scanner upgrade, scan date, and cohort differences, including these variables as covariates in our analyses. Although such statistical corrections are not optimal, our data and analyses were not initially designed to address our specific research questions, preventing us from fully eliminating potential confounding effects. Another issue arises from considering general intelligence as an explanatory factor for variations in executive function performance, which may impact the associations between cognitive measures and biomarkers. We decided not to include general IQ as a covariate, as it is challenging to disentangle its effects from the pervasive cognitive impairments characteristic of schizophrenia[95]. Consequently,

controlling for general IQ could undermine the statistical power needed to detect subtle effects of the illness[96]. Nonetheless, our results, while not necessarily generalizable, provide a valuable hypothesis-generating foundation for future studies aimed at exploring the complex relationship between cognitive functioning and both structural and functional networks in parallel.

Furthermore, the diffusion data were acquired using a single-shell, with a low b-value of 1000 s/mm^2 and 30 gradient directions. This may compromise the specificity to intra-axonal signals. However, studies using SSMT-CSD technique have shown that single-shell DWI data produces similar results compared to multi-shell DWI data[97]. The biological accuracy of single-shell data processed with CSD has also been confirmed in post-mortem histological studies[98]. We believe that the biological interpretation of our results conveys biologically relevant and reliable findings, even though they rely on less optimal data acquisition parameters.

DATA AVAILABILITY
The datasets generated and/or analyzed during the current study are available from the corresponding author upon reasonable request.

REFERENCES
1. Friston, K. J. & Frith, C. D. Schizophrenia: a disconnection syndrome? *Clin. Neurosci.* **3**, 89–97 (1995).
2. Andreasen, N. C. A unitary model of schizophrenia. *Arch. Gen. Psychiatry.* **56**, 781 (1999).
3. Nelson, B. G., Bassett, D. S., Camchong, J., Bullmore, E. T. & Lim, K. O. Comparison of large-scale human brain functional and anatomical networks in schizophrenia. *NeuroImage Clin.* **15**, 439–448 (2017).
4. Fornito, A. & Bullmore, E. T. Reconciling abnormalities of brain network structure and function in schizophrenia. *Curr. Opin. Neurobiol.* **30**, 44–50 (2015).
5. Voineskos, A. N. et al. Neuroimaging evidence for the deficit subtype of schizophrenia. *JAMA Psychiatry.* **70**, 472–480, https://doi.org/10.1001/jamapsychiatry.2013.786 (2013).
6. Holleran, L. et al. The relationship between white matter microstructure and general cognitive ability in patients with schizophrenia and healthy participants in the ENIGMA consortium. *Am. J. Psychiatry.* **177**, 537–547, https://doi.org/10.1176/appi.ajp.2019.19030225 (2020).
7. Kottaram, A. et al. Predicting individual improvement in schizophrenia symptom severity at 1-year follow-up: comparison of connectomic, structural, and clinical predictors. *Hum. Brain Mapp.* **41**, 3342–3357, https://doi.org/10.1002/hbm.25020 (2020).
8. Concha, L. A macroscopic view of microstructure: using diffusion-weighted images to infer damage, repair, and plasticity of white matter. *Neuroscience* **276**, 14–28, https://doi.org/10.1016/j.neuroscience.2013.09.004 (2014).
9. Jeurissen, B., Leemans, A., Tournier, J. D., Jones, D. K. & Sijbers, J. Investigating the prevalence of complex fiber configurations in white matter tissue with diffusion magnetic resonance imaging. *Hum. Brain Mapp.* **34**, 2747–2766, https://doi.org/10.1002/hbm.22099 (2013).
10. Raffelt, D. A. et al. Investigating white matter fibre density and morphology using fixel-based analysis. *Neuroimage* **144**, 58–73, https://doi.org/10.1016/j.neuroimage.2016.09.029 (2017).
11. Dhollander, T. et al. Fixel-based analysis of diffusion MRI: methods, applications, challenges and opportunities. *Neuroimage* **241**, 118417, https://doi.org/10.1016/j.neuroimage.2021.118417 (2021).
12. Jeurissen, B., Tournier, J. D., Dhollander, T., Connelly, A. & Sijbers, J. Multi-tissue constrained spherical deconvolution for improved analysis of multi-shell diffusion MRI data. *Neuroimage* **103**, 411–426, https://doi.org/10.1016/j.neuroimage.2014.07.061 (2014).
13. Rojas-Vite, G. et al. Histological validation of per-bundle water diffusion metrics within a region of fiber crossing following axonal degeneration. *Neuroimage* **201**, 116013, https://doi.org/10.1016/j.neuroimage.2019.116013 (2019).
14. Adanyeguh, I. M. et al. Autosomal dominant cerebellar ataxias: Imaging biomarkers with high effect sizes. *NeuroImage Clin.* **19**, 858–867, https://doi.org/10.1016/j.nicl.2018.06.011 (2018). June.

15. Pantelis, C. et al. Structural brain imaging evidence for multiple pathological processes at different stages of brain development in schizophrenia. *Schizophr. Bull.* **31**(3), 672–696, https://doi.org/10.1093/schbul/sbi034 (2005).

16. Bartholomeusz, C. F. et al. Structural neuroimaging across early-stage psychosis: aberrations in neurobiological trajectories and implications for the staging model. *Aust. N.Z. J. Psychiatry* **51**(5), 455–476, https://doi.org/10.1177/0004867416670522 (2017).

17. Stone, W. S. et al. Neurodegenerative model of schizophrenia: growing evidence to support a revisit.*Schizophr. Res.* **243**, 154–162, https://doi.org/10.1016/j.schres.2022.03.004 (2022).

18. Gupta, S. & Kulhara, P. What is schizophrenia: a neurodevelopmental or neuro-degenerative disorder or a combination of both A critical analysis. *Indian J. Psychiatry* **52**, 21–27, https://doi.org/10.4103/0019-5545.58891 (2010).

19. Kristensen, T. D. et al. Fibre density and fibre-bundle cross-section of the corti-cospinal tract are distinctly linked to psychosis-specific symptoms in anti-psychotic-naïve patients with first episode schizophrenia. *Eur. Arch. Psychiatry Clin. Neurosci.* **273**, 1797–1812 (2023).

20. Orellana, G. & Slachevsky, A. Executive functioning in schizophrenia. *Front. Psy-chiatry* **4**, 1–15, https://doi.org/10.3389/fpsyt.2013.00035 (2013). JUN.

21. Gilbert, S. J. & Burgess, P. W. Executive function. *Curr. Biol.* **18**, 110–114, https://doi.org/10.1016/j.cub.2007.12.014 (2008).

22. Fioravanti, M., Bianchi, V. & Cinti, M. E. Cognitive deficits in schizophrenia: an updated metanalysis of the scientific evidence. *BMC Psychiatry* **12**, 64, https://doi.org/10.1186/1471-244X-12-64 (2012).

23. Mesholam-Gately, R. I., Giuliano, A. J., Goff, K. P., Faraone, S. V. & Seidman, L. J. Neurocognition in first-episode schizophrenia: a meta-analytic review. *Neu-ropsychology.* **23**, 315–336, https://doi.org/10.1037/a0014708 (2009).

24. Szöke, A. et al. Tests of executive functions in first-degree relatives of schizo-phrenic patients: a meta-analysis. *Psychol Med.* **35**, 771–782, https://doi.org/10.1017/S0033291704003460 (2005).

25. Penades, R., Vallespi, L. G., Franck, N. & Dekerle, M. Neuroimaging studies of cognitive function in schizophrenia chapter. *Adv. Exp. Med. Biol.* **1118**, 117–134, https://doi.org/10.1007/978-3-030-05542-4_6 (2019). (January):v-vi.

26. Minzenberg, M. J., Laird, A. R., Thelen, S., Carter, C. S. & Glahn, D. C. Meta-analysis of 41 functional neuroimaging studies of executive function in schizophrenia. *Arch. Gen. Psychiatry* **66**, 811–822, https://doi.org/10.1001/archgenpsychiatry.2009.91 (2009).

27. Sui, J. et al. In search of multimodal neuroimaging biomarkers of cognitive def-icits in schizophrenia. *Biol. Psychiatry* **78**, 794–804 (2015).

28. Bojesen K. B., et al. Associations between cognitive function and levels of gluta-matergic metabolites and GABA in antipsychotic-naïve patients with schizophrenia or psychosis. *Biol Psychiatry.* https://doi.org/10.1016/j.biopsych.2020.06.027 (2020).

29. Nielsen, M. Ø. et al. Alterations of the brain reward system in antipsychotic nave schizophrenia patients. *Biol. Psychiatry.* **71**, 898–905 (2012).

30. Wing, J. K. et al. SCAN schedules for clinical assessment in neuropsychiatry. *Arch. Gen. Psychiatry* **47**, 589–593 (1990).

31. Kay, S. R., Fiszbein, A. & Opler, L. A. The positive and negative syndrome scale (PANSS) for schizophrenia. *Schizophr. Bull.* **13**, 261–276 (1987).

32. Kaneda, Y. et al. Measurement and treatment research to improve cognition in schizophrenia consensus cognitive battery: validation of the japanese version. *Psychiatry Clin. Neurosci.* **67**, 182–188 (2013).

33. Nelson, H. E. & O'Connell, A. Dementia: the estimation of premorbid intelligence levels using the New Adult Reading Test. *Cortex* **14**, 234–244 (1978).

34. Miyake, A. et al. The unity and diversity of executive functions and their con-tributions to complex "frontal lobe" tasks: a latent variable analysis. *Cogn. Psychol.* **41**, 49–100 (2000).

35. Friedman, NaomiP. & Miyake, A. Unity and diversity of executive functions: individual differences as a window on cognitive structure. *Cortex* **86**, 186–204 (2017).

36. Sahakian, B. J. & Owen, A. M. Computerized assessment in neuropsychiatry using CANTAB: Discussion paper. *J. R. Soc. Med.* **85**, 399–402 (1992).

37. Keefe, R. S. E. et al. Norms and standardization of the Brief Assessment of Cog-nition in Schizophrenia (BACS). *Schizophr. Res.* **102**, 108–115 (2008).

38. Puonti, O., Iglesias, J. E. & Van Leemput, K. Fast and sequence-adaptive whole-brain segmentation using parametric Bayesian modeling. *Neuroimage* **143**, 235–249 (2016).

39. Manjón, J. V. et al. Diffusion weighted image denoising using overcomplete local PCA. *PLoS One* **8**, e73021 (2013).

40. Tournier, J. D. et al. MRtrix3: A fast, flexible and open software framework for medical image processing and visualisation. *Neuroimage* **202**, 116137 (2019).

41. Andersson, J. L. R., Skare, S. & Ashburner, J. How to correct susceptibility distor-tions in spin-echo echo-planar images: application to diffusion tensor imaging. *Neuroimage* **20**, 870–888 (2003).

42. Jenkinson, M., Bannister, P., Brady, M. & Smith, S. Improved optimization for the robust and accurate linear registration and motion correction of brain images. *Neuroimage* **17**, 825–841 (2002).

43. Jenkinson, M., Beckmann, C. F., Behrens, T. E. J., Woolrich, M. W. & Smith, S. M. Fsl. *Neuroimage* **62**, 782–790 (2012).

44. Smith, S. M. et al. Advances in functional and structural MR image analysis and implementation as FSL. *Neuroimage* **23**, 208–219 (2004). S1SUPPL. 1.

45. Dhollander T., Raffelt D., Connelly A. Unsupervised 3-tissue response function estimation from single-shell or multi-shell diffusion MR data without a co-registered T1 image. In *Proc. ISMRM Workshop on Breaking the Barriers Diffusion MRI.* 2016;35:5. https://www.researchgate.net/publication/307863133_Unsupervised_3-tissue_response_function_estimation_from_single-shell_or_multi-shell_diffusion_MR_data_without_a_co-registered_T1_image

46. Raffelt, D. et al. Symmetric diffeomorphic registration of fibre orientation distribu-tions. *Neuroimage.* **56**, 1171–1180 (2011).

47. Raffelt, D. et al. Apparent Fibre Density: a novel measure for the analysis of diffusion-weighted magnetic resonance images. *Neuroimage* **59**, 3976–3994 (2012).

48. Smith, R. E., Tournier, J. D., Calamante, F. & Connelly, A. SIFT: spherical-deconvolution informed filtering of tractograms. *Neuroimage* **67**, 298–312 (2013).

49. Raffelt, D. A. et al. Connectivity-based fixel enhancement: whole-brain statistical analysis of diffusion MRI measures in the presence of crossing fibres. *Neuroimage* **117**, 40–55 (2015).

50. Smith, S. M. Fast robust automated brain extraction. *Hum. Brain Mapp.* **17**, 143–155 (2002).

51. Andersson J. L. R., Jenkinson M., Smith S. M. Non-linear optimisation. FMRIB technical report TR07JA1. http://fsl.fmrib.ox.ac.uk/analysis/techrep/tr07ja1/tr07ja1.pdf(FMRIB Centre JR Hospital, 2007).

52. Andersson J. L. R., Jenkinson M., Smith S. Non-linear registration, aka spatial nor-malisation. FMRIB Technial Report TR07JA2. Oxford Cent Funct Magn Reson Imaging Brain, https://doi.org/10.1016/j.neuroimage.2008.10.055 (Department of Clinical Neu-rolsciences, Oxford University, Oxford, UK. 2007).

53. Pruim, R. H. R. et al. ICA-AROMA: A robust ICA-based strategy for removing motion artifacts from fMRI data. *Neuroimage* **112**, 267–277 (2015).

54. Pruim, R. H. R., Mennes, M., Buitelaar, J. K. & Beckmann, C. F. Evaluation of ICA-AROMA and alternative strategies for motion artifact removal in resting state fMRI. *Neuroimage* **112**, 278–287 (2015).

55. Desikan, R. S. et al. An automated labeling system for subdividing the human cerebral cortex on MRI scans into gyral based regions of interest. *Neuroimage* **31**, 968–980 (2006).

56. Friston, K. J., Williams, S., Howard, R., Frackowiak, R. S. J. & Turner, R. Movement-related effects in fMRI time-series. *Magn. Reson. Med.* **35**, 346–355 (1996).

57. Nichols, T. & Holmes, A. Nonparametric permutation tests for functional neuroi-maging: a primer with examples. *Hum. Brain Mapp.* **15**, 1–25 (2001).

58. Mancuso, L. et al. The homotopic connectivity of the functional brain: a meta-analytic approach. *Sci. Rep.* **9**, 1–19 (2019).

59. Zuo, X. N. et al. Growing together and growing apart: regional and sex differences in the lifespan developmental trajectories of functional homotopy. *J. Neurosci.* **30**, 15034–15043 (2010).

60. Anderson, J. S. et al. Decreased interhemispheric functional connectivity in aut-ism. *Cereb Cortex* **21**, 1134–1146 (2011).

61. Mamah, D. et al. Anterior thalamic radiation integrity in schizophrenia: a diffusion-tensor imaging study. *Psychiatry Res.* **183**, 1–7 (2010).

62. Roy, D. S. et al. Anterior thalamic dysfunction underlies cognitive deficits in a subset of neuropsychiatric disease models. *Neuron* **109**, 2590–2603.e13 (2021).

63. Jiang, Y., Patton, M. H. & Zakharenko, S. S. A case for thalamic mechanisms of schizophrenia: perspective from modeling 22q11.2 deletion syndrome. *Front. Neural Circuits* **15**, 1–16 (2021). December.

64. Mukherjee, A. & Halassa, M. M. The associative thalamus: a switchboard for cor-tical operations and a promising target for schizophrenia. *Neuroscientist* **30**, 132–147 (2024).

65. Best, J. R. & Miller, P. H. A developmental perspective on executive function. *Child. Dev.* **81**, 1641–1660 (2010).

66. Guo, J. Y. et al. Predicting psychosis risk using a specific measure of cognitive control: a 12-month longitudinal study. *Psychol. Med.* **50**, 1–10 (2020).

67. Ramsay, I. S., Mueller, B., Ma, Y., Shen, C. & Sponheim, S. R. Thalamocortical connectivity and its relationship with symptoms and cognition across the psy-chosis continuum. *Psychol. Med.* **53**, 5582–5591 (2023).

68. Ribolsi, M., Daskalakis, Z. J., Siracusano, A. & Koch, G. Abnormal asymmetry of brain connectivity in schizophrenia. *Front. Hum. Neurosci.* **8**, 1–11 (2014). DEC.

69. Zhu, F. et al. Functional asymmetry of thalamocortical networks in subjects at ultra-high risk for psychosis and first-episode schizophrenia. *Eur. Neuropsycho-pharmacol.* **29**, 519–528 (2019).

70. Saito, J. et al. Can reduced leftward asymmetry of white matter integrity be a marker of transition to psychosis in at-risk mental state? *Asian J. Psychiatr.* **54**, 102450 (2020).

71. Hua, J. et al. Altered functional connectivity between sub-regions in the thalamus and cortex in schizophrenia patients measured by resting state BOLD fMRI at 7T. *Schizophr. Res.* **206**, 370–377 (2019).

72. Mittal, P. K., Mehta, S., Solanki, R. K. & Swami, M. K. A comparative study of cognitive flexibility among first episode and multi-episode young schizophrenia patients. *Ger. J. Psychiatry* **16**, 130–136 (2013).

73. Uddin, L. Q. Cognitive and behavioural flexibility: neural mechanisms and clinical considerations. *Nat. Rev. Neurosci.* **22**, 1–13 (2021).

74. Waltz, J. A. The neural underpinnings of cognitive flexibility and their disruption in psychotic illness. *Neuroscience* **345**, 203–217 (2017).

75. Kim, S. E., Jung, S., Sung, G., Bang, M. & Lee, S. H. Impaired cerebro-cerebellar white matter connectivity and its associations with cognitive function in patients with schizophrenia. *npj Schizophr.* **7**, 38 (2021).

76. Sacks, D. D. et al. White matter integrity according to the stage of mental disorder in youth. *Psychiatry Res. Neuroimaging* **307**, 111218 (2021).

77. Wang, Y., Hu, X. & Li, Y. Investigating cognitive flexibility deficit in schizophrenia using task-based whole-brain functional connectivity. *Front. Psychiatry.* **13**, 1–9 (2022).

78. Dajani, D. R. & Uddin, L. Q. Demystifying cognitive flexibility: Implications for clinical and developmental neuroscience. *Trends Neurosci.* **38**, 571–578 (2015).

79. Knyazeva M. G. Splenium of corpus callosum: patterns of interhemispheric interaction in children and adults. *Neural Plast.* 2013. https://doi.org/10.1155/2013/639430 (2013).

80. Van Den Heuvel, M. P., Mandl, R. C. W., Kahn, R. S. & Hulshoff Pol, H. E. Functionally linked resting-state networks reflect the underlying structural connectivity architecture of the human brain. *Hum. Brain Mapp.* **30**, 3127–3141 (2009).

81. Booth, R., Wallace, G. L. & Happé, F. Connectivity and the corpus callosum in autism spectrum conditions. Insights from comparison of autism and callosal agenesis. *Prog. Brain Res.* **189**, 303–317 (2011).

82. Eccher, M. Corpus callosum. *Encycl. Neurol. Sci.* **1**, 867–868 (2014).

83. Luders, E. et al. Positive correlations between corpus callosum thickness and intelligence. *Neuroimage* **37**, 1457–1464 (2007).

84. Crespi, B. & Badcock, C. Psychosis and autism as diametrical disorders of the social brain. *Behav. Brain Sci.* **31**, 241–320 (2008).

85. Yeager, B. E. et al. Central precuneus lesions are associated with impaired executive function. *Brain Struct. Funct.* **227**, 3099–3108 (2022).

86. Wenderoth, N., Debaere, F., Sunaert, S. & Swinnen, S. P. The role of anterior cingulate cortex and precuneus in the coordination of motor behaviour. *Eur. J. Neurosci.* **22**, 235–246 (2005).

87. Vatansever, D., Manktelow, A. E., Sahakian, B. J., Menon, D. K. & Stamatakis, E. A. Cognitive flexibility: a default network and basal ganglia connectivity perspective. *Brain Connect.* **6**, 201–207 (2016).

88. Utevsky, A. V., Smith, D. V. & Huettel, S. A. Precuneus is a functional core of the default-mode network. *J. Neurosci.* **34**, 932–940 (2014).

89. Guo, W. et al. Hyperactivity of the default-mode network in first-episode, drug-naive schizophrenia at rest revealed by family-based case-control and traditional case-control designs. *Medicines* **96**, e6223 (2017).

90. Hu, M. L. et al. A review of the functional and anatomical default mode network in schizophrenia. *Neurosci Bull.* **33**, 73–84 (2017).

91. Mashal, N., Vishne, T. & Laor, N. The role of the precuneus in metaphor comprehension: evidence from an fMRI study in people with schizophrenia and healthy participants. *Front Hum Neurosci.* **8**, 1–11 (2014).

92. Gray, C. M. The temporal correlation hypothesis of visual feature integration: still alive and well. *Neuron* **24**, 31–47 (1999).

93. FitzGibbon, L., Cragg, L. & Carroll, D. J. Primed to be inflexible: the influence of set size on cognitive flexibility during childhood. *Front. Psychol.* **5**, 1–13 (2014).

94. Jahanshad, N. et al. Multi-site genetic analysis of diffusion images and voxelwise heritability analysis: a pilot project of the ENIGMA–DTI working group. *Neuroimage* **81**, 455–469 (2013). NOvennber.

95. Kahn, R. S. & Keefe, R. S. E. Schizophrenia is a cognitive illness: time for a change in focus. *JAMA Psychiatry* **70**, 1107–1112 (2013).

96. Miller, G. A. & Chapman, J. P. Misunderstanding analysis of covariance. *J. Abnorm. Psychol.* **110**, 40–48 (2001).

97. Aerts H., Dhollander T., Marinazzo D. Evaluating the performance of 3-tissue constrained spherical deconvolution pipelines for within-tumor tractography. *bioRxiv*. Published online 2019.

98. Smith, R. E., Tournier, J. D., Calamante, F. & Connelly, A. The effects of SIFT on the reproducibility and biological accuracy of the structural connectome. *Neuroimage* **104**, 253–265, https://doi.org/10.1016/j.neuroimage.2014.10.004 (2015).

AUTHOR CONTRIBUTIONS

Tina D. Kristensen (T.D.K.), Karen S. Ambrosen (K.S.A.), and Jayachandra M. Raghava (J.M.R.) conceived the research questions and performed the modelling. T.D.K., K.S.A., J.M.R. carried out the analyses. Kirsten B. Bojesen (K.B.B.), Mette Ø. Nielsen (M.Ø.N.), Cecilie K. Lemvigh (C.K.L.) contributed to data collection and sample preparation. Thijs Dhollander (T.D.H.), Anita D. Barber (A.D.B.), Egill Rostrup (ER), Birgitte Fagerlund (B.F.), supervised the methods used. Birte Y. Glenthøj (B.Y.G.), Bjørn H. Ebdrup (B.H.E.), Christos Pantelis (C.P.) contributed to the interpretation of the results. T.D.K. took the lead in writing the manuscript. All authors provided critical feedback and helped shape the research, analysis and manuscript.

COMPETING INTERESTS

B.H.E. is part of the Advisory Board of Eli Lilly Denmark A/S, Janssen-Cilag, Lundbeck Pharma A/S, and Takeda Pharmaceutical Company Ltd; and has received lecture fees from Bristol-Myers Squibb, Otsuka Pharma Scandinavia AB, Eli Lilly Company, and Lundbeck Pharma A/S. K.B.B. received lecture fees from Lundbeck Pharma A/S.

ADDITIONAL INFORMATION

Supplementary information The online version contains supplementary material available at https://doi.org/10.1038/s41537-024-00487-9.

Correspondence and requests for materials should be addressed to Tina D. Kristensen.

Reprints and permission information is available at http://www.nature.com/reprints

Publisher's note Springer Nature remains neutral with regard to jurisdictional claims in published maps and institutional affiliations.